Am J Physiol Heart Circ Physiol 309: H276–H284, 2015.
First published May 22, 2015; doi:10.1152/ajpheart.00164.2015.

CALL FOR PAPERS | *Cardiovascular Responses to Environmental Stress*

Load-dependent extracellular matrix organization in atrioventricular heart valves: differences and similarities

S. Hamed Alavi,[1,2] Aditi Sinha,[1,2] Earl Steward,[3] Jeffrey C. Milliken,[3] and Arash Kheradvar[1,2]

[1]*The Edwards Lifesciences Center for Advanced Cardiovascular Technology, University of California, Irvine, Irvine, California;* [2]*Department Biomedical Engineering, University of California, Irvine, Irvine, California; and* [3]*Division of Cardiothoracic Surgery, University of California, Irvine, Irvine, California*

Submitted 9 March 2015; accepted in final form 17 May 2015

Alavi SH, Sinha A, Steward E, Milliken JC, Kheradvar A. Load-dependent extracellular matrix organization in atrioventricular heart valves: differences and similarities. *Am J Physiol Heart Circ Physiol* 309: H276–H284, 2015. First published May 22, 2015; doi:10.1152/ajpheart.00164.2015.—The extracellular matrix of the atrioventricular (AV) valves' leaflets has a key role in the ability of these valves to properly remodel in response to constantly varying physiological loads. While the loading on mitral and tricuspid valves is significantly different, no information is available on how collagen fibers change their orientation in response to these loads. This study delineates the effect of physiological loading on AV valves' leaflets microstructures using Second Harmonic Generation (SHG) microscopy. Fresh natural porcine tricuspid and mitral valves' leaflets (n = 12/valve type) were cut and prepared for the experiments. Histology and immunohistochemistry were performed to compare the microstructural differences between the valves. The specimens were imaged live during the relaxed, loading, and unloading phases using SHG microscopy. The images were analyzed with Fourier decomposition to mathematically seek changes in collagen fiber orientation. Despite the similarities in both AV valves as seen in the histology and immunohistochemistry data, the microstructural arrangement, especially the collagen fiber distribution and orientation in the stress-free condition, were found to be different. Uniaxial loading was dependent on the arrangement of the fibers in their relaxed mode, which led the fibers to reorient in-line with the load throughout the depth of the mitral leaflet but only to reorient in-line with the load in deeper layers of the tricuspid leaflet. Biaxial loading arranged the fibers in between the two principal axes of the stresses independently from their relaxed states. Unlike previous findings, this study concludes that the AV valves' three-dimensional extracellular fiber arrangement is significantly different in their stress-free and uniaxially loaded states; however, fiber rearrangement in response to the biaxial loading remains similar.

collagen fibers; mechanics; uniaxial load; biaxial load

NEW & NOTEWORTHY

This study delineates the effect of physiological loading on atrioventricular heart valves' leaflets microstructures using Second Harmonic Generation microscopy. The presented data help understanding the biomechanical responses of the AV valves to the load, and facilitate the development of more accurate and sophisticated constitutive models for native valve leaflets.

Address for reprint requests and other correspondence: A. Kheradvar, The Edwards Lifesciences Center for Advanced Cardiovascular Technology, Univ. of California, Irvine, 2410 Engineering Hall, Irvine, CA 92697 (e-mail: arashkh@uci.edu).

THE MITRAL AND TRICUSPID HEART valves, referred to as atrioventricular (AV) valves, control the blood flow between the atria and ventricles of the heart. Regurgitation is the most common type of AV valve disease with a 1.7% prevalence of mitral regurgitation (MR), which is the highest among all types of valvular disease in the United States (18, 34). In its primary form, MR usually results from the valves leaflets' pathological weakening and gross changes in their extracellular matrix (ECM) that are referred to as myxomatous degeneration (1, 17, 22). Alternatively, functional MR leads to stiffer leaflets and abnormal ECM remodeling (23).

Contrary to mitral valve regurgitation, functional tricuspid regurgitation (TR) is the most common form of TR, and is often associated with left-sided valve disease mainly due to MR (10, 25, 42). This shows that regardless of the valve type, the ECM characteristics of AV valves' leaflets have a key role in the pathophysiology of these valves. The composition, arrangement, and structural organization of AV valves' ECM are influenced by the mechanics of the left and right heart during development and maturation as well as by load dependence tissue remodeling (24, 38).

Mitral and tricuspid valves are anatomical equivalents of each other, and both possess annulus, leaflets, chordae tendinae, and papillary muscles. From an anatomical perspective, the tricuspid valve has a larger orifice with three thinner and more translucent leaflets, whereas the mitral valve is bileaflet and its anterior and posterior leaflets are relatively thicker. Both valves' leaflets are composed of a smooth endocardial layer consisting of endothelial cells and a fibrous skeleton with spongiosa and fibrosa layers that are mostly composed of collagen fibers (21, 38, 41). Mitral and tricuspid valves are shown to have their fibers arranged in radial and circumferential directions (11, 29, 38).

The leaflets' microstructure determines its nonlinear stress-strain (20, 35, 43) and anisotropic characteristics (9, 36, 43) that influence leaflet functionality. Collagen fibers, in particular, play a crucial role in providing structural integrity to withstand the cyclic loads during systole and diastole by constant stretching and relaxation. It is well-known that the mechanical response to cyclic loads is determined by the ability of collagen fibers to orient in the direction of the principal stresses applied to the leaflet (15, 16, 40). This necessitates accurate characterization of the valvular ECM and its remodeling potential under loading conditions. While loading conditions on mitral and tricuspid valves are significantly different due to the pressure difference in the left and right ventricles, no informa-

tion exists on how collagen fibers change orientation in response to these stresses. This study intends to delineate the AV valves' differences and similarities in collagen fiber orientation in response to mechanical loading conditions. The results should help better understanding the AV valves' pathophysiology.

MATERIALS AND METHODS

Sample Preparation

Fresh porcine mitral and tricuspid heart valves (n = 12/type of valve) were obtained at the University of California Irvine (UCI) Department of Surgery (The UCI Institutional Animal Care and Use Committee no. 1999-1712) and stored at 4°C in phosphate-buffered saline with 2% mixture of antibiotics including penicillin, streptomycin, and amphotericin B (GIBCO, Carlsbad, CA). The valves' leaflets were excised and prepared for Second Harmonic Generation (SHG) microscopy. The tissue segments remained hydrated before and during the microscopy using the above-mentioned solution.

Biaxial Mechanical Loading Setup

To provide real-time monitoring of biaxial loads applied over a thin tissue segment mounted on the stage of a high-resolution nonlinear microscope, a biaxial mechanical loading device (Fig. 1*A*) was developed as described in detail in our previous publication (5). In a few words, this lightweight device consists of four loading grips connected to adapters for clamping the tissue, one stage insert, one platform, four pulleys, four tension screws, and four force gauges. The entire device was placed on the motorized *X–Y* stage on a Zeiss LSM 510 Meta Multiphoton microscope (Carl Zeiss Microscopy). The force extended on each grip was monitored in real time using four digital force gauges with 50 mN resolution (Mecmesin, West Sussex, UK). In a near-frictionless situation, small pulleys guide the thin cables from grips to the corresponding force gauges. To achieve tension control, small grips held the tissue specimen at all four sides of the tissue segments. Tension control was achieved by placing a 10–32 screw between each grip and its corresponding force gauge in a way that screw rotation increased tension in the cable. The force reading was calibrated by applying an initial pretension with a typical value of 0.15 N.

Loading/Imaging Experiment

SHG images were acquired by a Zeiss LSM 510 Meta Multiphoton microscope. The microscope is equipped with a Ti:Sapphire, Chameleon-Ultra (Coherent, Santa Clara, CA) femtosecond laser source tunable from 690 to 1,040 nm. SHG excitation and emission filtration was set to 900 and 450–465 nm, respectively. Experiments were performed on three different regions on the belly part (Fig. 1, *B* and *C*) of the mitral and tricuspid valve leaflets (n = 12/type of valve).

The radial direction of the leaflet was identified as the direction of the conventional x-axis in the x–y image plane (Fig. 1*C*). SHG image stacks with the field of view of 225 × 225 μm were acquired for each segment. The imaging was performed from the surface of the leaflets up to 60 μm deep inside the tissue under four different loading conditions. At the beginning of the experiment, the leaflets were imaged under low initial tension to determine the collagen fiber orientation in the relaxed state, which was then used to normalize the changes of the collagen fiber orientation under uniaxial and biaxial loading conditions. Following the baseline imaging, the leaflets were subjected to uniaxial radial loading and biaxial loading. Any displacement of the leaflet tissue was avoided while applying the loading conditions during imaging. The tensile forces of 1.4 and 0.5 N were applied to mitral and tricuspid valve leaflets, respectively. These values are equivalent to the tensile forces experienced by a native leaflet in the porcine heart (19). Finally, the leaflets were unloaded and imaged again.

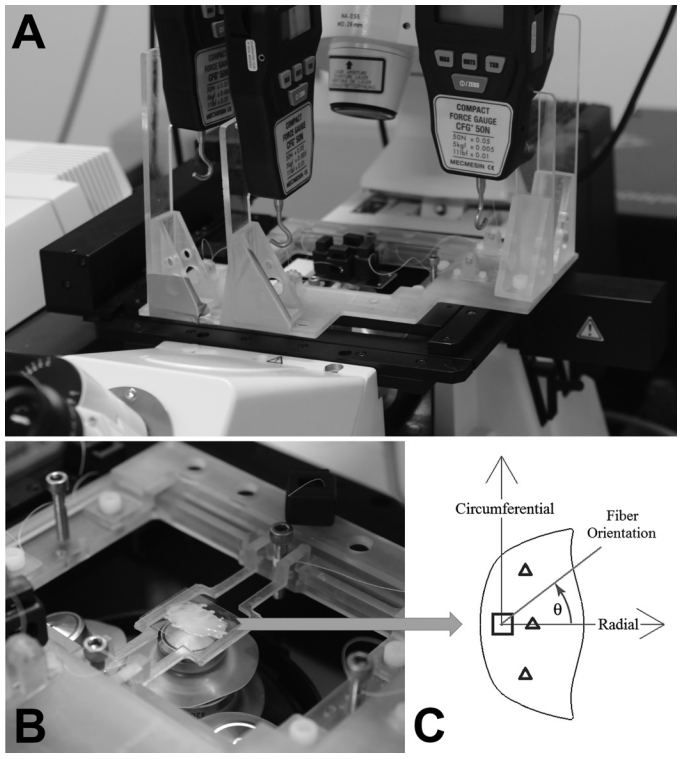

Fig. 1. The custom-made biaxial testing device mounted on the stage of a standard multiphoton microscope. *A*: the biaxial system was designed to apply controlled uni- and biaxial tensile stresses to the tissue segments simultaneous with the imaging. The lightweight system fits into the *X–Y* scanning stage of the microscope, and through using a pulley system the exerted force on each side of the specimen is transferred to the force gauges. The magnitude of the forces is controlled using four screws placed between the grips connected to the specimen and the force gauges. *B*: the sample tissue placed on the stage of the microscope-compatible biaxial tester. The tissue was placed in a specific orientation so that the uniaxial radial and biaxial tensile forces can be applied in accordance of the radial and circumferential directions of the leaflet. *C*: schematic representation that demonstrates the radial and circumferential directions and the calculated fiber orientation angle on a sample leaflet drawing. The imaging experiment was performed at three different regions in the belly of the leaflet that are shown with red triangles. The tensile forces of 1.4 and 0.5 N were applied to multiple samples of mitral and tricuspid valve leaflets, respectively.

Image Analysis

SHG image stacks were processed to extract mean collagen bundle direction from each image. The algorithms were all previously developed and validated in-house using a MATLAB code (Mathworks) implementing two-dimensional (2D) Fourier Transform analysis (5, 6). The frequencies of light-intensity oscillation for pixels were calculated and rearranged to bring the zero frequency to the center of the image. An intensity threshold was defined as the mean value plus three SDs to suppress the background of Fourier images by thresholding (7). The frequency indexes of the filtered images were extracted and plotted. To calculate the mean fiber direction, a regression line was defined through the distribution of frequencies, and then fiber direction was extracted orthogonal to this trend. The Fourier Transform allows characterization of the frequency of light-intensity fluctuations for each pixel. Thus, it was possible to obtain the distribution of frequencies related to the spacing of the collagen fibers.

Histology and Immunohistochemistry

Histology was performed by placing the leaflets in formalin. Paraffinized sections (5 μm) were stained by hematoxylin and eosin (H&E) as well as Masson's trichrome for general morphology and ECM collagen components, respectively. To assess the cellular phenotypes, immunohistochemistry was performed by incubation with monoclonal mouse antibodies for α-smooth muscle actin (α-SMA), vimentin, and CD31. DAB Chromogen substrate was used with Mayer's hematoxylin counterstain. A secondary biotin-labeled goat anti-mouse IgG antibody was used for incubation before the signal developed. Normal light microscopy was used to analyze all the staining.

Statistical Analysis

The data were derived from the SHG images in triplets and at three different regions of the belly of the leaflet tissues (Fig. 1*C*); they are reported as means ± SD. A total of 24 valves were used (n = 12/valve type); therefore, 36 series of images and 108 series of data for mitral valves and the same number for tricuspid valves were obtained. An unpaired Student's t-test was performed for statistical analysis using the R software package for Windows (Lucent Technologies, Costa Mesa, CA). A P value of <0.05 was considered statistically significant.

RESULTS

Histological Studies

The results for histology and immunohistochemistry on both mitral and tricuspid valves are presented in Fig. 2. H&E staining shows an organized structure for both valves with uniform cell densities (Fig. 2, *A* and *B*), whereas trichrome staining (Fig. 2, *C* and *D*) demonstrates a distinct collagenous fibrosa layer in tricuspid compared with mitral. In mitral leaflet, the collagen fibers were found abundantly present at almost all layers; however, in tricuspid leaflets the collagen concentration was found much higher at the fibrosa compared with the spongiosa layer. Immunohistochemistry data were found quite similar in both valves with low levels of α-SMA-positive cells (Fig. 2, *E* and *F*). These cells were not distributed evenly in both valves. However, they tend to be more distributed in the spongiosa layer rather than fibrosa. Endothelial lining was observed by CD31 staining (Fig. 2, *G* and *H*), and the level of vimentin-positive cells was reported high in both valves (Fig. 2, *I* and *J*).

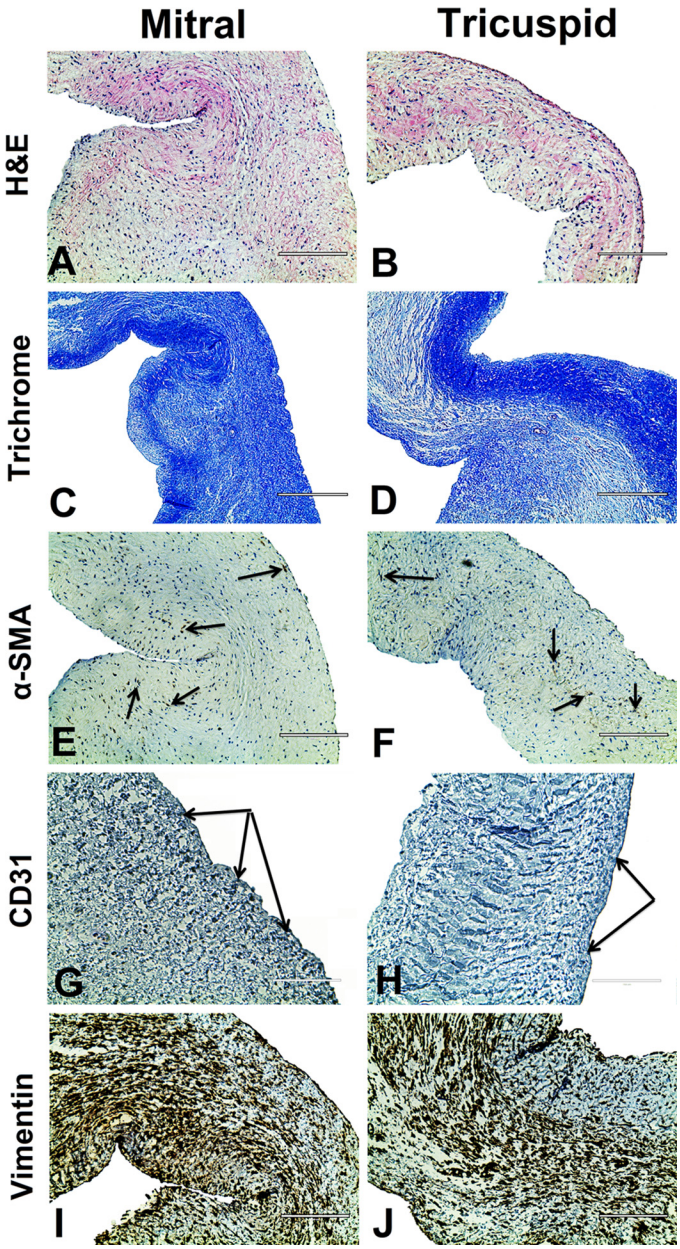

Fig. 2. Histology and immunohistochemistry of the native mitral and tricuspid valve leaflets. The first column displays the results for the mitral valve and the second column for the tricuspid valve. Hematoxylin and eosin (H&E) (*A* and *B*) revealed similar structure with uniform cell density (scale bars: 200 μm), but Masson's trichrome (*C* and *D*) showed different distribution for collagen components (scale bars: 400 μm). Immunohistochemistry for α-smooth muscle actin (α-SMA, *E* and *F*) with scale bars = 200 μm, CD31 (*G* and *H*) with scale bars = 100 μm, and vimentin (*I* and *J*) with scale bars = 200 μm demonstrates quite similar data with low amounts of α-SMA (brown color shown by arrows)- and high amounts of vimentin-positive cells. CD31-positive (endothelial) cells are also identified by arrows as the lining layer of the leaflets.

Loading-Imaging Studies

Mitral valve. Figure 3 shows the matrix map of a mitral anterior leaflet at the 10-, 40-, and 60-μm depths throughout the tissue before loading and under uniaxial radial and biaxial loading regimes. The ECM map of the unloading states appeared identical to the relaxed states (SHG data not shown). A varying configuration of the fibers for the relaxed state through the depth in the leaflet's belly can be observed. The fibers tend to arrange almost radially at the superficial layers (i.e., <30 μm depth) and circumferentially at the deeper layers (i.e., deeper than 30 μm). Once loaded radially, the fibers reorient densely along with the load at all depths. The collagen bundles also become thicker compared with the relaxed state but not fully stretched. This is somehow different when the leaflets were subjected to biaxial loading, where the fibers changed to a stretched and completely straight configuration, as can be seen in Fig. 3; the fibers reoriented in between the two principal axes of the loads.

The comparisons of angle of orientation vs. depth at which the images were taken are shown in Figs. 4 and 5 for uniaxial radial and biaxial loadings, respectively. Each figure reports the relaxed, loading, and unloading cases. The mean bundle direction in relaxed states for the superficial layers is 3.7 ±

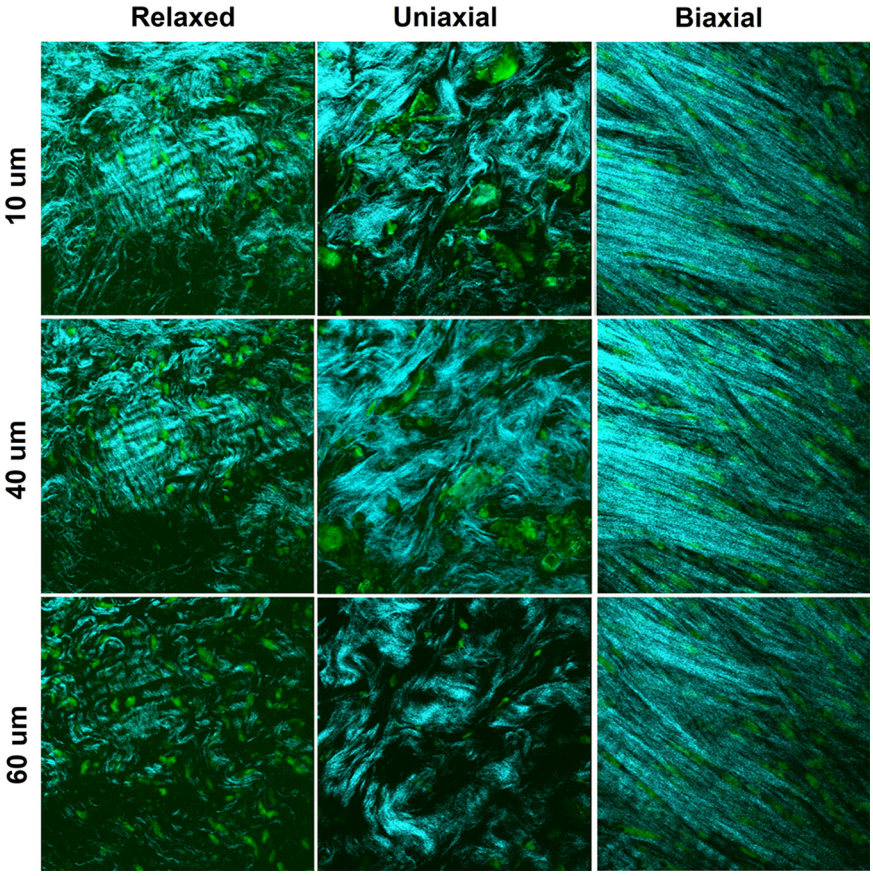

Fig. 3. Collagen fiber distributions of the mitral valve leaflet taken by loading-imaging technique described. It displays the changes in the orientation of collagen fibers for relaxed, uniaxial radial, and biaxial loadings at 10, 40, and 60 μm deep inside the tissue. The unloading images have not been shown. As can be seen, collagen fiber orientation changes profoundly during the loading condition.

1.1°; however, there is a sudden change in the fiber orientation for deeper layers where the fiber mean orientation is 65.7 ± 2.8°. Fourier analysis indicates that uniaxial radial loading reorients all fibers between 4° and 10° with an average of 6.5 ± 0.9°, whereas biaxial loading reorients them between 45° and 51° with an average of 47.7 ± 1.6°, almost in between the two principal axes of the loads as observed in the SHG images. Unloading rapidly redirected the fibers to a position similar to their relaxed state for both uniaxial and biaxial cases with $P \sim 0.83$ and 0.71, respectively.

Tricuspid valve. The ECM configuration of a fresh porcine tricuspid leaflet at the depths of 10, 40, and 60 μm in relaxed and under uniaxial radial and biaxial loadings are shown in Fig. 6. SHG images of unloading states are not shown, since they were similar to the relaxed states. An unorganized configuration for the fibers can be observed in the relaxed states; the superficial fibers, in contrast to the ones observed in mitral leaflets, tend to be more directed in between the radial and circumferential directions. They slightly turn toward the circumferential direction at deeper layers, as also observed in the mitral leaflets. However, the uniaxial radial response was found to be different compared with mitral leaflet with collagen fibers aligning with the radial load only at deeper layers. The superficial layers seem unaffected under the load by remaining at their relaxed

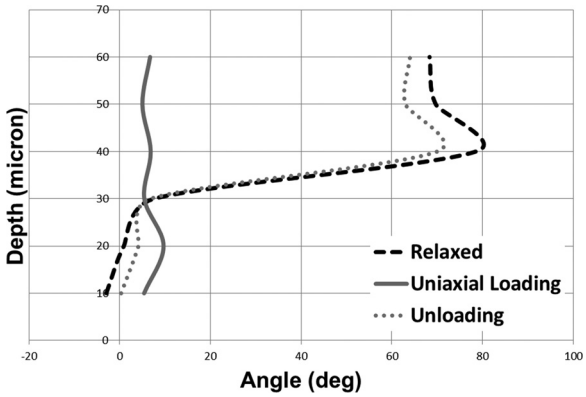

Fig. 4. Comparison of collagen fiber orientation in relaxed, uniaxial radial loading, and unloading states of the mitral valve leaflet. Uniaxial radial loading shows that fibers are oriented in-line with the direction of the load.

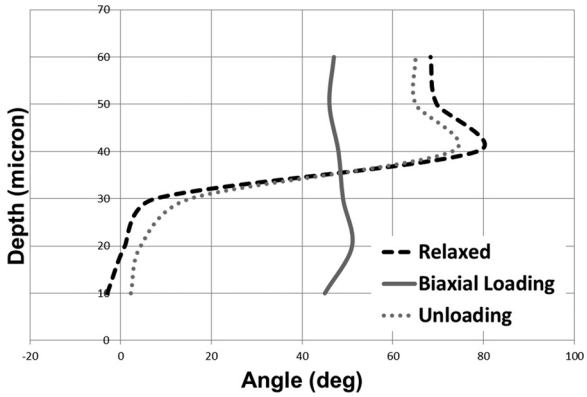

Fig. 5. Comparison of collagen fiber orientation in relaxed, biaxial loading, and unloading states of the mitral valve leaflet. Biaxial loading shows that fibers are oriented in between the two principal axes of the loads.

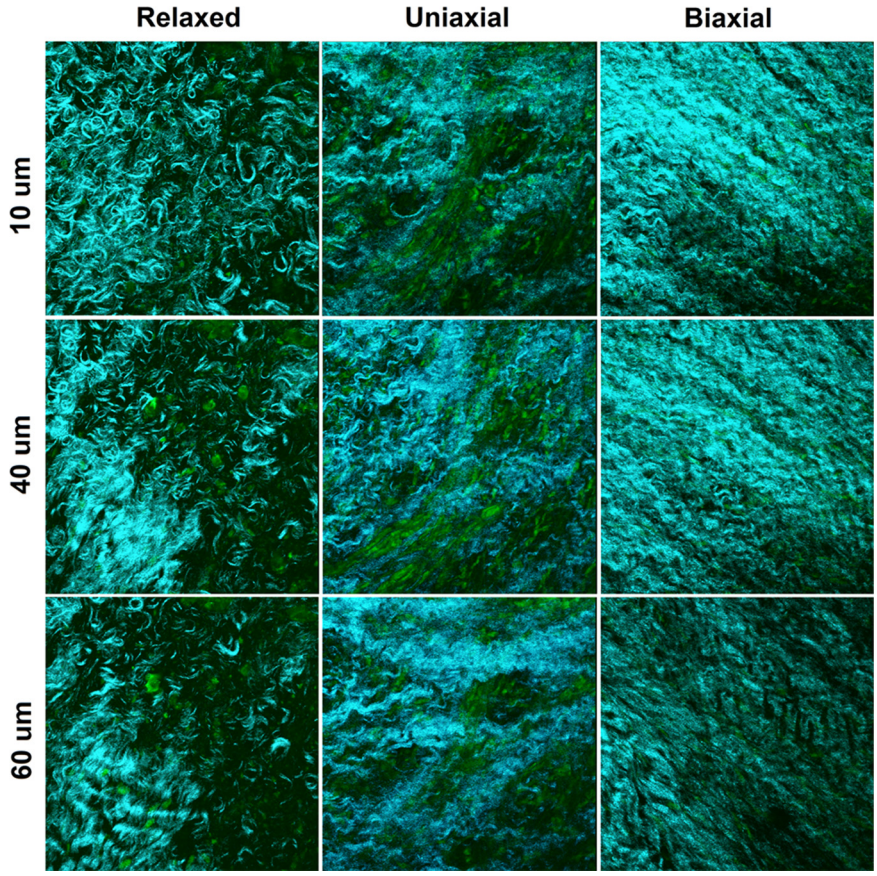

Fig. 6. Collagen fiber distributions of the tricuspid valve leaflet taken by loading-imaging technique described. It displays the changes in the orientation of collagen fibers for relaxed, uniaxial radial, and biaxial loadings at 10, 40, and 60 μm deep inside the tissue. The unloading images have not been shown. As can be seen, collagen fiber orientation changes profoundly during the loading condition.

original configuration, whereas the biaxial response was found to be similar to the mitral valve with fibers aligning in between the two principal axes of the stress. The types of fibers clearly look different with a thicker and straighter shape in mitral vs. a wavier form with little curls in tricuspid (Figs. 3 and 6).

Figures 7 and 8 illustrate the average fiber orientation angle vs. the depth of imaging for uniaxial radial and biaxial loadings, respectively. Each figure compares the data acquired for relaxed, loading, and unloading conditions. The relaxed states show a variation of mean fiber direction from 23° to 81° throughout the tissue depth. This demonstrates that the fibers are scattered in a smaller angle (~58°) once compared with the mitral leaflet (~83°). Uniaxial radial loading slightly turns the superficial fibers ~4° toward the circumferential direction (~5° for mitral leaflet) and reorient them at 29.8 ± 2.0° (compared with 6.8 ± 0.7° for mitral). Deeper inside the tissue, the fibers stand in between −6° and 1° with an average of −3.6 ± 0.4°(compared with 6.1 ± 0.6° for mitral), almost aligned with the radial load. This shows that the radial force acts similarly in both AV valves and tends to make the deep fibers aligned with the force while turning the superficial fibers slightly toward the circumferential direction. Still, only in mitral leaflets and not tricuspids, the fibers are redirected all aligned with

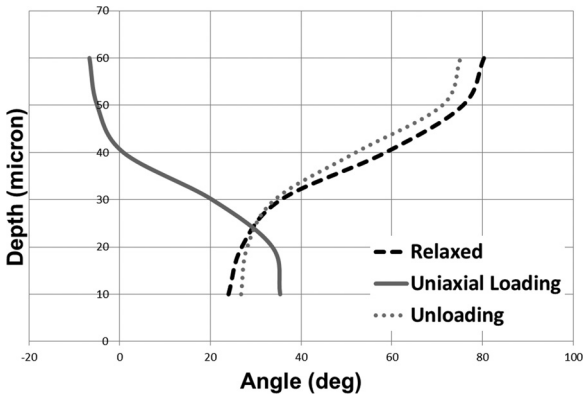

Fig. 7. Comparison of collagen fiber orientation in relaxed, uniaxial radial loading, and unloading states of the tricuspid valve leaflet. Uniaxial radial loading shows that fibers are oriented in-line with the direction of the load only at deeper layers but not at the surface.

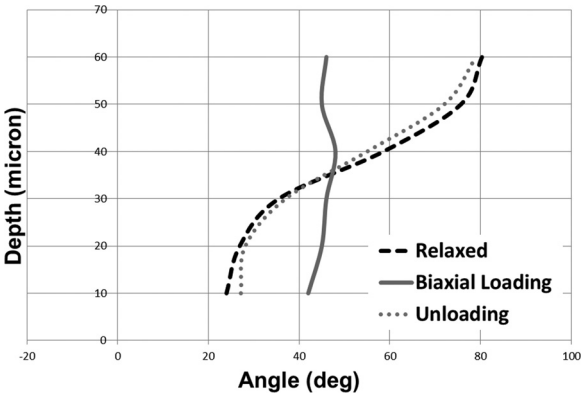

Fig. 8. Comparison of collagen fiber orientation in relaxed, biaxial loading, and unloading states of the tricuspid valve leaflet. Biaxial loading shows that fibers are oriented in between the two principal axes of the loads.

the load. The biaxial response is analogous ($P \sim 0.08$) to the mitral leaflet with fibers reorienting in between 42° and 48° with an average of 45.3 ± 1.9°. Unloading cases return the fibers to a position similar to their relaxed states for both uni- and biaxial conditions with P values of ~0.79 and 1.05, respectively. This information has been summarized in Table 1 to compare the microstructure of mitral and tricuspid valves at different conditions.

DISCUSSION

Studying the heart valves' ECM remodeling is crucial for understanding their physiological functions, their modes of failure, and for identifying congenital abnormalities during their development and function. This knowledge would also help in designing better prosthetic or tissue-engineered heart valves. There are several previous studies describing the role of collagen fiber architecture in either a native or a bioprosthetic heart valve (9, 12–14, 44). However, it is not known how these fibers change their spatial orientation under physiological cyclic loading. In other words, microstructural changes in collagen fibers during valve function in vivo are not well studied. These adjustments are extremely important in defining the biomechanical response of the tissue to the varying degree of stresses in a cardiac cycle. Any disruption of the extracellular organization of the leaflets, especially collagen fiber orientation, during development or later in adulthood due to a disease process may lead to structural and morphological abnormalities such as thickening, stiffening, or valve leakage. In this study, for the first time, we investigated the temporal and spatial changes in the pattern of the collagen fibers in native AV leaflets based on a novel simultaneous loading-imaging technique.

The AV valves are similar in their gross anatomy and microscopic histology, yet they are subject to different mechanical loading environments (38). During systole when the ventricular pressure reaches up to or greater than 100 mmHg in the LV, the mitral valve remains closed and therefore experiences significant hydrostatic pressure that can be fairly modeled with a biaxial loading system. This pressure change is much less dramatic in the right ventricle with a systolic pressure range of ~15 to ~30 mmHg. These differences in the hemodynamics of the left and right ventricles would affect the leaflets' microstructures during development and maturation, allowing them to adapt to their environment. This study delineates these difference by assessing the AV leaflets' microscopic histology and their fiber arrangement in their relaxed mode (both cases are considered nearly stress-free conditions) compared with the loaded modes.

The Stress-Free Condition

Although the histology and immunohistochemistry data show minimal differences between the two valves, the tricuspid valves' leaflets have considerably nonhomogenous collagen distributions with a distinct and more collagenous fibrosa layer than mitral leaflets, which can affect their mechanical response to the load (Fig. 2). Grashow et al. showed that the mechanical responses of mitral leaflets are strain-independent and have minimal hysteresis (20). This nonlinear stress-strain relationship has been reported by May-Newman and Yin (36) and Liao et al. (33). This strain independency has been rationalized based on collagen fiber recruitment theories (31, 32). Reduced collagen concentration in a diseased mitral valve was observed by Kunzelman et al. and led to increased tissue stiffness as well as reduced coaptation (30). However, there is currently no study showing the differences between collagen fiber orientation in mitral leaflets with a lower concentration gradient and tricuspid leaflets with a higher gradient, in terms of their functions and their mechanical responses to the load. Based on the rule of mixtures, it is anticipated that such a collagen distribution in mitral leaflets can ensure the proper closure of the valves and strengthen their resistance to higher levels of pressure during systole. Additionally, our data suggest that the collagen fibers in mitral valves' leaflets are generally thicker but straighter than the ones observed in tricuspid valves (Figs. 3 and 6), which should enhance their mechanical resilience in accordance with the previous statement.

The SHG data showed a significantly different ($P \sim 0.004$) configuration of the fibers in the superficial layers of the relaxed modes. The fibers in the deeper layers seem to orient in a similar fashion ($P \sim 0.93$). No significant differences were observed between fiber orientations of the valves from different animals with $P \sim 0.23$ and 0.51 for the mitral and tricuspid

Table 1. *Comparison of mitral and tricuspid valves in stress-free and loaded conditions*

	Sress-Free Condition							Loaded Condition			
	Histology		Immunohistochemistry			Relaxed		Uniaxial		Biaxial	
	H&E	Trichrome	α-SMA	CD31	Vimentin	Superficial	Deep	Superficial	Deep	Superficial	Deep
Mitral valve	Organized structure with uniform cell density	Fibrosa: rich in collagen content Spongiosa: lower amount of collagen	−	+	+	Radial	Inclined-toward circumferential direction	Radial	Radial	Inclined, in the middle of the two axes	Inclined, in the middle of the two axes
Tricuspid valve	Organized structure with uniform cell density	Fibrosa: rich in collagen content Spongiosa: poor in collagen content	−	+	+	Inclined, toward radial direction	Circumferential	Inclined, toward radial direction	Radial	Inclined, in the middle of the two axes	Inclined, in the middle of the two axes

valves, respectively. During the relaxed state, the fibers are scattered in a smaller angle in the tricuspid valve than in the mitral valve. This might be due to the similar flow profiles of both valves, but to lower velocities in the tricuspid (almost two-thirds), due to its larger orifice, which lowers the shear stress on the surface during valve opening (2, 46). The radial fiber orientation on the surface and the circumferential fiber direction in deeper layers would give the mitral valve leaflet enough compliance to resist the surface shear stresses that are damaging to superficial layers of the leaflet. Therefore, this predefined configuration of the fibers created during valve development and maturation is key to describing valves' mechanical responses to different hemodynamic conditions in the left and right heart. This would also define the heterogeneous and anisotropic properties of the valves seen in other studies (36, 43).

The Loaded Condition

According to the results from the uniaxial radial loading experiment, both valves' responses were similar in nature other than the fact that the collagen fibers in the mitral valve align in the direction of the load regardless of their position while the fibers in the tricuspid valve only align with the load in deeper layers. By comparing the loaded condition with the relaxed mode, we infer that the uniaxial radial load cannot significantly change the orientation of the fibers in superficial layers; however, it dramatically shifts the deeper layers' fiber orientation to a direction almost perpendicular to their original direction. We found that the uniaxial loading results for both valves were dependent on the fibers' orientation in their relaxed mode. This arrangement would give mitral leaflets better extensibility that allows them to accommodate greater tensile loads than tricuspid leaflet. Lower tensile stress due to lower hydrostatic pressure in the right ventricle would cause the fibers in the tricuspid valve to not align with the unidirectional load at all layers. This may also change the shape of the collagen fibers in the tricuspid leaflet to be thinner than and not as straight as the fibers in the mitral leaflet (Figs. 3 and 6). There is also a possibility that the different mechanical responses in mitral and tricuspid valves are due to the differences in their specific collagen type contents. However, because the dominant and the load-bearing type of collagen in heart valves is type I collagen, we believe this factor would not significantly affect the ECM orientation of these tissues under the load.

We observed that the biaxial responses of both valves are quite similar and independent from their relaxed modes with fibers standing in between the two principal axes of the stresses in all layers. This ideal situation mimics the closure of the valve where the AV valves experience tensile forces under hydrostatic pressure of the right or left ventricles during end-diastole. However, when the blood flows and produces shear stress on the surface of the leaflets, the situation will change. In this case, the optimal response is varied depending on the type of the valve and the loading environment, as observed in our results. Therefore, unlike previous thoughts, the differentiating factor between mitral and tricuspid valves is their mechanical response to the load once they are at their opening state and not when they are closed. The unloading response in all the samples confirmed that there is no viscoplastic behavior or permanent change in fiber orientation, which is in accordance with the work done by other groups (20, 43). There are structural constitutive models for planar collagenous tissues such as the one developed by Sacks (39) that considers the experimentally derived fiber orientation. However, in all these models the spatial distribution of fibers is an important missing factor. Incorporating the findings of the present study into these constitutive models should better portray the mechanical characteristics of the valve.

It should be mentioned that the microstructure of the valve leaflets is not composed of only collagen but elastin and glycoaminoglycans components (Fig. 9); however, the mechanical response of the leaflet to the load is mainly affected by the collagen fiber distribution and orientation. This means that the collagen can be considered as the main determinant of the valve's microstructure. The collagen-rich layers of both valves are in the fibrosa layer that has the highest level of collagen concentration, which, according to our study, was found almost similar in both valves. Moreover, the fibrosa layer is the main load-bearing component of the leaflet and defines its mechanical characteristics (28, 37, 45), which makes it more critical to study its load-dependent behavior. Nevertheless, we observed that there were minimal differences in the fiber orientation in different regions of the leaflets at the same depth where the collagen concentration was found different. This may imply that, on an inner layer parallel to the leaflet's surface, the differences in collagen density would not significantly influence a change in fiber orientation as can be seen in Fig. 9. Although we did not test it, we anticipate that this statement can also be extended to the layers perpendicular to the leaflet surface since the fibers' direction would not change the individual fibers' characteristics and the biomechanical response of the tissue as a whole. Due to the structure of AV valves' collagen fibers, their changes in fiber direction can be more of a compensatory response to the type of the applied load and not to the collagen concentration. Therefore, we think that the collagen fibers in the spongiosa layer in lower concentration (a.k.a. the fiber orientation in deeper layers) would still show similar fiber orientation under the load. Accordingly, it is anticipated that the viscoelastic mechanical properties of these layers in both valves would be completely different from the fibrosa layer.

Impact on Tissue-Engineered Heart Valves

The present data can be used as a model in defining the microstructural response of the leaflet tissue to uniaxial and biaxial loads. By implementing these models, an optimal way to engineer a valve can be described considering the three-dimensional (3D) fiber orientations. Almost all of the computational and constitutive models use a 2D scheme for defining fiber orientation, which may not be accurate considering the spatial sensitivity of the fibers to the load. Here we anticipate that, by implementing the optimal fiber orientation data, one can improve bioprosthetic and tissue-engineered valves' durability and functionality. Our results indicate that the uniaxial response of the native leaflets in deeper layers is quite similar to the uniaxial response of the bovine pericardial leaflets used in bioprosthetic valves (5). However, the superficial layers' fiber orientation, which is a key determinant of the leaflet's response to shear stress during valve opening, is somehow different in bovine pericardial tissues from their orientation in

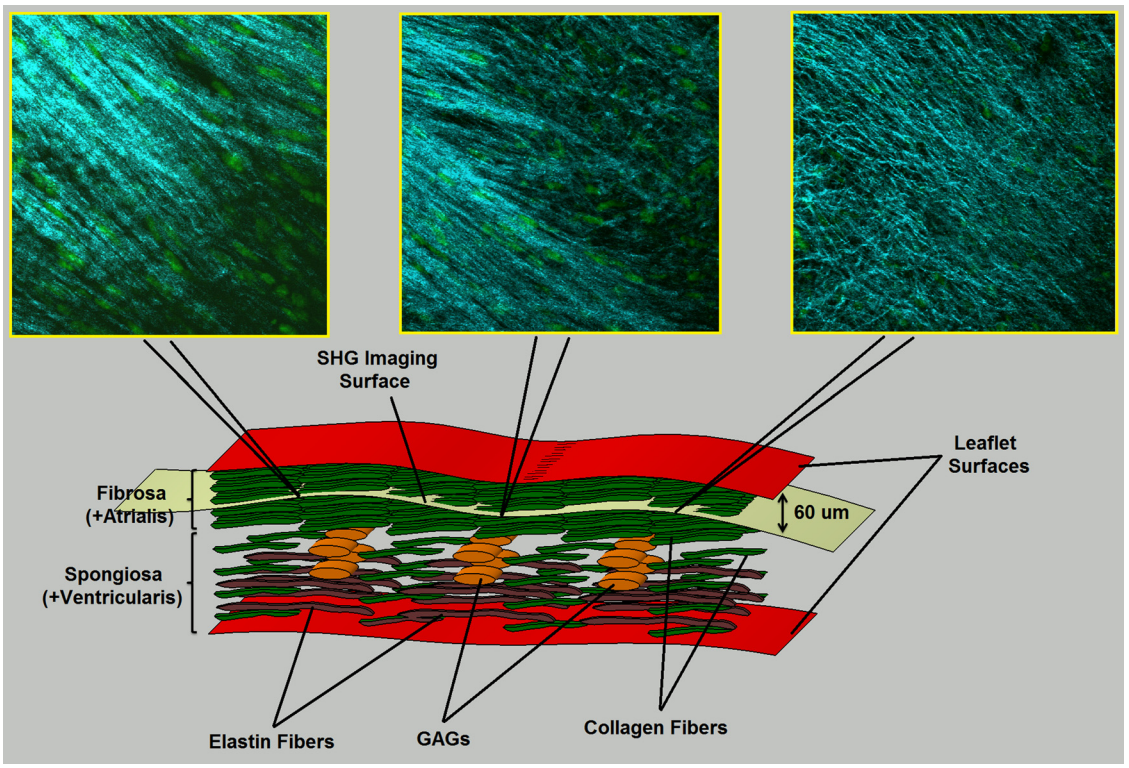

Fig. 9. Schematic representation of a cross section of a heart valve leaflet shows the layered fashion of the tissue with all the extracellular matrix components. Elastin (brown), collagen (green), and glycoaminoglycans (GAGs, orange) are distributed in the fibrosa and spongiosal layers. The fibrosa layer is rich in collagen fibers and more suitable for studying the load-dependent tissue remodeling. The Second Harmonic Generation images at the *top* were taken at the same depth (60 μm) from the surface of tissue inside the fibrosa. These images display different collagen density but almost similar fiber orientation on a plane parallel to the surface of the leaflet.

native valves. The biaxial response of the native leaflets is also different from the response of pericardial tissues with fibers arranged ~45° in native valves and ~60° in pericardial tissues (5). Because in the circumferential direction valves are less extensible than they are in the radial direction (8), it was expected to see in response to the biaxial load the native valve fibers reorient closer to the axis where stiffness is higher. This observation might be due to the differences in the anisotropic properties of native and fixed pericardial leaflets (43), which can be used as a reference for designing more durable bioprosthetic heart valves. The observed differences between the superficial and deeper collagen fibers suggest that the decellularization process of the heart valves for tissue engineering purposes (26) should be performed carefully not to damage the native fiber configuration of the most superficial layers. A gentle but longer decellularization process to reach the deeper layers would be particularly beneficial for mitral valves since the alignment of its fibers will significantly influence its response to shear stress during valve opening.

In conclusion, we have characterized the ECM organization of the AV valves in both stress-free and loaded conditions. In the stress-free state, we observed that not only the collagen distribution is significantly different in mitral and tricuspid valves, but their fiber orientation is also different in 3D. In the uniaxial loading state the fibers in both valves rearranged differently in a configuration dependent on their relaxed states. The biaxial response of the valves was quite similar and found independent of their relaxed configuration. The present data would help in understanding the biomechanical response of the AV valves to the load to develop more accurate constitutive models and to design naturally comparable tissue-engineered and bioprosthetic heart valves. We believe this study is a first step in analysis of the pathological situations such as in mitral prolapse, myxomatous disease, and other structural AV valve diseases. This may also help in optimizing material properties used in prosthetic or tissue-engineered heart valves (3, 4, 27).

Limitations

Due to the limited depth penetration of multiphoton techniques within turbid tissues, optical sectioning deeper than 60 μm was not possible. Additionally, there might have been a slight dislocation between the relaxed, loading, and unloading phases, which we tried to minimize.

ACKNOWLEDGMENTS

We thank the histology laboratory at the University of California Irvine (UCI) School of Medicine for assisting us in performing the histology and immunohistochemistry of the samples. We also thank the Sue and Bill Gross Stem Cell Research Center at UCI for providing facilities to perform the multiphoton microscopies and the related experiments.

GRANTS

This work is partially supported by a grant from Children's Heart Foundation and one from Edwards Lifesciences Foundation.

DISCLOSURES

No conflicts of interest, financial or otherwise, are declared by the authors.

AUTHOR CONTRIBUTIONS

Author contributions: S.H.A., A.S., E.S., and J.C.M. performed experiments; S.H.A. analyzed data; S.H.A., A.S., and A.K. interpreted results of experiments; S.H.A. prepared figures; S.H.A. and A.S. drafted manuscript; S.H.A. and A.K. edited and revised manuscript; A.K. and S.H.A. conception and design of research; A.K. approved final version of manuscript.

REFERENCES

1. **Akhtar S, Meek KM, James V.** Ultrastructure abnormalities in proteoglycans, collagen fibrils, and elastic fibers in normal and myxomatous mitral valve chordae tendineae. *Cardiovasc Pathol* 8: 191–201, 1999.
2. **Alam M, Wardell J, Andersson E, Samad BA, Nordlander R.** Characteristics of mitral and tricuspid annular velocities determined by pulsed wave Doppler tissue imaging in healthy subjects. *J Am Soc Echocardiogr* 12: 618–628, 1999.
3. **Alavi SH, Groves EM, Kheradvar A.** The effects of transcatheter valve crimping on pericardial leaflets. *Ann Thoracic Surg* 97: 1260–1266, 2014.
4. **Alavi SH, Kheradvar A.** Metal mesh scaffold for tissue engineering of membranes. *Tissue Eng* 18: 293–301, 2011.
5. **Alavi SH, Ruiz V, Krasieva T, Botvinick EL, Kheradvar A.** Characterizing the collagen fiber orientation in pericardial leaflets under mechanical loading conditions. *Ann Biomed Eng* 41: 547–561, 2013.
6. **Alavi SH, Sinha A, Kheradvar A.** Matrix remodeling in native atrioventricular valves' leaflets in response to mechanical loading (Abstract). *Circulation* 130: A12281, 2014.
7. **Ambekar. Ramachandra Rao R, Mehta MR, Leithem S, Toussaint JKC.** Fourier transform-second-harmonic generation imaging of collagen fibers in biological tissues. In: *Biomedical Optics and 3-D Imaging*. Miami, FL: Optical Society of America, 2010, p. BSuD63.
8. **Balguid A, Rubbens MP, Mol A, Bank RA, Bogers AJ, van Kats JP, de Mol BA, Baaijens FP, Bouten CV.** The role of collagen cross-links in biomechanical behavior of human aortic heart valve leaflets–relevance for tissue engineering. *Tissue Eng* 13: 1501–1511, 2007.
9. **Billiar KL, Sacks MS.** Biaxial mechanical properties of the natural and glutaraldehyde treated aortic valve cusp-part I: experimental results. *J Biomechan Eng* 122: 23–30, 2000.
10. **Carpentier A, Deloche A, Hanania G, Forman J, Sellier P, Piwnica A, Dubost C, McGoon D.** Surgical management of acquired tricuspid valve disease (Abstract). *J Thorac Cardiovasc Surg* 67: 53, 1974.
11. **Cochran R, Kunzelman K, Chuong C, Sacks M, Eberhart R.** Nondestructive analysis of mitral valve collagen fiber orientation (Abstract). *ASAIO J* 37: M447, 1991.
12. **De Hart J, Peters G, Schreurs P, Baaijens F.** Collagen fibers reduce stresses and stabilize motion of aortic valve leaflets during systole. *J Biomechan* 37: 303–311, 2004.
13. **Doehring T, Kahelin M, Vesely I.** Mesostructures of the aortic valve. *J Heart Valve Dis* 14: 679–686, 2005.
14. **Driessen NJ, Boerboom RA, Huyghe JM, Bouten CV, Baaijens FP.** Computational analyses of mechanically induced collagen fiber remodeling in the aortic heart valve. *J Biomechan Eng* 125: 549–557, 2003.
15. **Driessen NJ, Cox MA, Bouten CV, Baaijens FP.** Remodelling of the angular collagen fiber distribution in cardiovascular tissues. *Biomechan Model Mechanobiol* 7: 93–103, 2008.
16. **Driessen NJB, Peters GWM, Huyghe JM, Bouten CVC, Baaijens FPT.** Remodelling of continuously distributed collagen fibres in soft connective tissues. *J Biomechan* 36: 1151–1158, 2003.
17. **Freed LA, Levy D, Levine RA, Larson MG, Evans JC, Fuller DL, Lehman B, Benjamin EJ.** Prevalence and clinical outcome of mitral-valve prolapse. *N Engl J Med* 341: 1–7, 1999.
18. **Go AS, Mozaffarian D, Roger VL, Benjamin EJ, Berry JD, Blaha MJ, Dai S, Ford ES, Fox CS, Franco S.** Heart disease and stroke statistics–2014 update: a report from the American Heart Association (Abstract). *Circulation* 129: e28, 2014.
19. **Grande KJ, Cochran R, Reinhall P, Kunzelman K.** Stress variations in the human aortic root and valve: the role of anatomic asymmetry. *Ann Biomed Eng* 26: 534–545, 1998.
20. **Grashow J, Yoganathan A, Sacks M.** Biaixal stress-stretch behavior of the mitral valve anterior leaflet at physiologic strain rates. *Ann Biomed Eng* 34: 315–325, 2006.
21. **Gross L, Kugel M.** Topographic anatomy and histology of the valves in the human heart (Abstract). *Am J Pathol* 7: 445, 1931.
22. **Hayek E, Gring CN, Griffin BP.** Mitral valve prolapse. *Lancet* 365: 507–518, 2005.
23. **He S, Fontaine AA, Schwammenthal E, Yoganathan AP, Levine RA.** Integrated mechanism for functional mitral regurgitation leaflet restriction versus coapting force: in vitro studies. *Circulation* 96: 1826–1834, 1997.
24. **Hinton RB, Yutzey KE.** Heart valve structure and function in development and disease. *Annu Rev Physiol* 73: 29–46, 2011.
25. **Izumi C, Iga K, Konishi T.** Progression of isolated tricuspid regurgitation late after mitral valve surgery for rheumatic mitral valve disease. *J Heart Valve Dis* 11: 353–356, 2002.
26. **Kheradvar A, Groves E, Dasi L, Alavi SH, Tranquillo R, Grande-Allen KJ, Simmons C, Griffith B, Falahatpisheh A, Goergen C, Mofrad MK, Baaijens F, Little S, Canic S.** Emerging trends in heart valve engineering. Part I. Solutions for future. *Ann Biomed Engineer* 43: 833–843, 2015.
27. **Kheradvar A, Groves E, Goergen C, Alavi SH, Tranquillo R, Simmons C, Dasi L, Grande-Allen KJ, Mofrad MK, Falahatpisheh A, Griffith B, Baaijens F, Little S, Canic S.** Emerging trends in heart valve engineering. Part II. Novel and standard technologies for aortic valve replacement. *Ann Biomed Engineer* 43: 844–857, 2015.
28. **Kunzelman K, Cochran R, Murphree S, Ring W, Verrier E, Eberhart R.** Differential collagen distribution in the mitral valve and its influence on biomechanical behaviour. *J Heart Valve Dis* 2: 236–244, 1993.
29. **Kunzelman KS, Cochran R.** Stress/strain characteristics of porcine mitral valve tissue: parallel versus perpendicular collagen orientation. *J Card Surg* 7: 71–78, 1992.
30. **Kunzelman KS, Quick DW, Cochran RP.** Altered collagen concentration in mitral valve leaflets: biochemical and finite element analysis. *Ann Thoracic Surg* 66: S198–S205, 1998.
31. **Lanir Y.** Constitutive equations for fibrous connective tissues. *J Biomechan* 16: 1–12, 1983.
32. **Lanir Y.** A structural theory for the homogeneous biaxial stress-strain relationships in flat collagenous tissues. *J Biomechan* 12: 423–436, 1979.
33. **Liao J, Yang L, Grashow J, Sacks MS.** The relation between collagen fibril kinematics and mechanical properties in the mitral valve anterior leaflet. *J Biomechan Eng* 129: 78–87, 2007.
34. **Maganti K, Rigolin VH, Sarano ME, Bonow RO.** Valvular heart disease: diagnosis and management. In: *Mayo Clinic Proceedings*. New York, NY: Elsevier, 2010, p. 483–500.
35. **May-Newman K, Yin F.** A constitutive law for mitral valve tissue. *J Biomechan Eng* 120: 38–47, 1998.
36. **May-Newman K, Yin FC.** Biaxial mechanical behavior of excised porcine mitral valve leaflets. *Am J Physiol Heart Circ Physiol* 269: H1319–H1327, 1995.
37. **McCarthy KP, Ring L, Rana BS.** Anatomy of the mitral valve: understanding the mitral valve complex in mitral regurgitation. *Eur J Echocardiogr* 11: i3–i9, 2010.
38. **Misfeld M, Sievers HH.** Heart valve macro-and microstructure. *Phil Trans Royal Soc B Biol Sci* 362: 1421–1436, 2007.
39. **Sacks MS.** Incorporation of experimentally-derived fiber orientation into a structural constitutive model for planar collagenous tissues. *J Biomechan Eng* 125: 280–287, 2003.
40. **Sacks MS, Smith DB, Hiester ED.** The aortic valve microstructure: effects of transvalvular pressure. *J Biomed Materials Res* 41: 131–141, 1998.
41. **Schoen FJ.** Evolving concepts of cardiac valve dynamics: the continuum of development, functional structure, pathobiology, and tissue engineering. *Circulation* 118: 1864–1880, 2008.
42. **Spinner EM, Shannon P, Buice D, Jimenez JH, Veledar E, Pedro J, Adams DH, Yoganathan AP.** In vitro characterization of the mechanisms responsible for functional tricuspid regurgitation. *Circulation* 124: 920–929, 2011.
43. **Stella JA, Liao J, Sacks MS.** Time-dependent biaxial mechanical behavior of the aortic heart valve leaflet. *J Biomechan* 40: 3169–3177, 2007.
44. **Tower TT, Tranquillo RT.** Alignment maps of tissues. II. Fast harmonic analysis for imaging. *Biophys J* 81: 2964–2971, 2001.
45. **Vesely I, Noseworthy R.** Micromechanics of the fibrosa and the ventricularis in aortic valve leaflets. *J Biomechan* 25: 101–113, 1992.
46. **Yoganathan A.** Heart valve dynamics. *Biomechanics: Principles and applications*.